Extended Abstracts of the 2005 International Conference on Solid State Devices and Materials, Kobe, 2005, pp.850-851

A-8-2

Ta-based metal gates (Ta, TaB_x, TaN_x and TaC_x) -Modulated Work Function and Improved Thermal Stability-

Reika Ichihara, Yoshinori Tsuchiya, Yuuichi Kamimuta, Masato Koyama, and Akira Nishiyama

Advanced LSI Technology Laboratory, Toshiba Corp.
8, Shinsugita-cho, Isogo-ku, Yokohama 235-8522, Japan
Phone: +81-45-770-3667 Fax: +81-45-770-3578 E-mail:reika.ichihara@toshiba.co.jp

1. Introduction

Integration of dual metal gate with minimum change of CMOS device fabrication process is enormous challenge; different metals with suitable effective work function ($\Phi_{m\text{-}eff}$) for n-type and p-type MISFET complicates fabrication process. From this point of view, we focused on $\Phi_{m\text{-}eff}$ control using same metal-based compounds. In this paper, we investigated $\Phi_{m\text{-}eff}$ and thermal stability of Ta-based metal (Ta, TaB_x, TaN_x or TaC_x) /SiO_2 or HfSiON stack structures systematically. As a result, $\Phi_{m\text{-}eff}$ changes from 4.4 eV (Ta) to 4.8 eV (TaC_x) owing to the influence of constituents properties. We report TaC_x is a promising candidate for p-type MISFET metal gate applicable to the conventional CMOS process flow.

2. Experimental

Ta-based metals were deposited on SiO_2/p-Si or HfSiON/SiO_2/p-Si to fabricate MIS capacitors. Deposition of Ta alloy films were performed by sputtering of Ta, TaB, Ta_2N or TaC targets in Ar atmosphere. Deposited films show reasonably low resistivity values of approximately 100 $\mu\Omega$ cm (Fig. 1). To examine thermal stability of these stack structures, some samples were annealed at 800ºC for 30 min, or at 1000ºC for 20 s followed by forming gas annealing (FGA) at 450ºC for 30 min. The C-V characteristics were measured at a frequency of 100 kHz. These samples were analyzed by TEM, back-side XPS and UPS.

3. Results and discussion

A. Modulated $\Phi_{m\text{-}eff}$ and improved thermal stability of Ta-based gate electrodes

Fig. 2 shows that C-V curves for MIS capacitors with Ta-compounds shift to positive direction from that of pure Ta, implying $\Phi_{m\text{-}eff}$ increase for alloyed materials. From y-intercepts of V_{fb}-T_{eff} relationships, we extract $\Phi_{m\text{-}eff}$ without the influence of fixed charges (Fig. 3). $\Phi_{m\text{-}eff}$ values change from 4.4eV (pure Ta) to 4.8 eV (TaC_x). Fig. 4 shows that $\Phi_{m\text{-}eff}$ is dependent on their electronegativities, suggesting that higher electronegativity of B, N, or C than that of Ta brings about $\Phi_{m\text{-}eff}$ modulation.

As far as the conventional CMOS process flow is concerned, metal gate electrodes need to be stable under S/D activation condition. In TaB_x samples after high temperature annealing, increased capacitance at inversion region suggests that boron penetration through SiO_2 into the channel region occurs (not shown). Fig. 5 shows that $\Phi_{m\text{-}eff}$ of TaN_x and TaC_x are quite stable through 1000ºC annealing, while $\Phi_{m\text{-}eff}$ of Ta increases to 4.6 eV after the annealing. TEM observation (Fig. 6) reveals that Ta reacts heavily with SiO_2 and interfacial layer (I.L.) forms at 1000ºC. The I.L. contains Ta, Si and O (EDX, data not shown). We also found that tiny crystal grains are involved in the I.L. (Fig. 7). Electron diffraction analysis reveals that these crystalline precipitates are TaO_x or $TaSi_x$ (not shown). We believe that such reaction layer is responsible for the undesirable $\Phi_{m\text{-}eff}$ increase after 1000ºC annealing (Fig. 5). In contrast, there is no reaction layer between TaN_x or TaC_x and SiO_2 even after 1000ºC annealing (Fig. 6). It is clear that the suppression of the interface reaction in the case of TaN_x and TaC_x leads to the superior $\Phi_{m\text{-}eff}$ stability (Fig. 5).

Although it is reported that $\Phi_{m\text{-}eff}$ of many gate electrode materials on high-k insulator are different from that on SiO_2,[1] $\Phi_{m\text{-}eff}$ value of 4.9~5.0 eV for TaC_x/HfSiON is obtained (Fig. 8), which is close to that of TaC_x/SiO_2. In addition, $\Phi_{m\text{-}eff}$ does not change even after 1000ºC annealing (Fig. 8). Thermal stability of TaC_x/HfSiON structure is also confirmed by TEM image (Fig. 9), suggesting that the $\Phi_{m\text{-}eff}$ stability stems from the chemically inert nature of the TaC_x/HfSiON interface.

B. Clarification of crucial factors that affect $\Phi_{m\text{-}eff}$ for TaC_x/dielectric interfaces

With regard to TaC_x, vacuum work function ($\Phi_{m\text{-}vac}$) and $\Phi_{m\text{-}eff}$ near to E_c have been reported,[2],[3] which are much smaller than our $\Phi_{m\text{-}eff}$. So we carefully clarify the possible factors that influence $\Phi_{m\text{-}eff}$ value. Firstly we certify the composition of our TaC_x film, because excess C cause $\Phi_{m\text{-}eff}$ to move toward $\Phi_{m\text{-}vac}$ of C (5.0 eV)[4]. Fig.10 shows depth profiles of Ta and C in the TaC_x film measured by RBS. Profiles are almost flat and the average C/Ta ratio is 0.9 (+/-0.1). If C atoms accumulate at the TaC_x/dielectric interface, $\Phi_{m\text{-}eff}$ would also reflect the $\Phi_{m\text{-}vac}$ of C. To check this, Si-substrate was removed from the TaC_x/SiO_2/Si and angle resolved XPS from the SiO_2 side was practiced. XPS C1s spectrum shows a peak of C-Ta bonding in TaC_x beneath SiO_2 layer (Fig.11). The Ta/C ratio, which is estimated from peak areas of Ta-C (C1s) and Ta4d, shows weak dependence on take-off angle (TOA) (Fig.12). This means that the C pile up never occurs in our specimen. Effect of dipoles at the metal/dielectric interface on $\Phi_{m\text{-}eff}$ value should also be considered. We examined $\Phi_{m\text{-}vac}$ of our TaC_x film by means of ultraviolet photoelectron spectroscopy (UPS). $\Phi_{m\text{-}vac}$ for the Ta film is also evaluated as a reference. As shown in Fig.13, $\Phi_{m\text{-}vac}$ for the TaC_x is higher than that of Ta, and their discrepancy (0.22 eV) is slightly smaller than that in $\Phi_{m\text{-}eff}$ (0.4 eV, Fig.3). This result indicates that interface dipoles increase the TaC_x $\Phi_{m\text{-}eff}$ to some extent. However, the main cause of our high $\Phi_{m\text{-}eff}$ value for TaC_x/dielectrics is $\Phi_{m\text{-}vac}$ of the TaC_x. The reason for the difference between our $\Phi_{m\text{-}vac}$ and reported values is under investigation.

3.2 Conclusion

Effective work function and thermal stability of MIS structures with Ta and Ta-compounds electrodes have been investigated systematically. In Ta-compounds, $\Phi_{m\text{-}eff}$ change of +0.4 eV and improved thermal stability are obtained. Relatively high $\Phi_{m\text{-}eff}$ of TaC_x gate (4.8~5.0 eV) on both SiO_2 and HfSiON is mainly due to high vacuum work function of the film. We suggest that tantalum carbide with excellent thermal stability is a promising p-type MISFET electrode.

References

[1] Y.-C. Yeo et al., IEEE EDL., vol.23, (2002) P342
[2] G. R. Gruzalski et al., Surf. Sci., vol.239, (1990) L517
[3] J.K. Schaeffer et al., IEDM2004, P287
[4] H.B. Michaelson et al., J. Appl. Phys., Vol.48, (1977) P4729

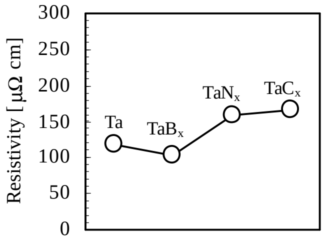

Fig. 1. Resistivities of Ta and Ta-compounds.

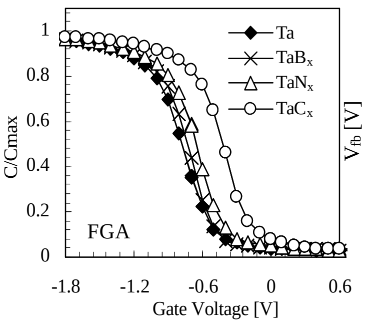

Fig. 2. C-V characteristics of Ta-based gate/SiO_2 capacitors.

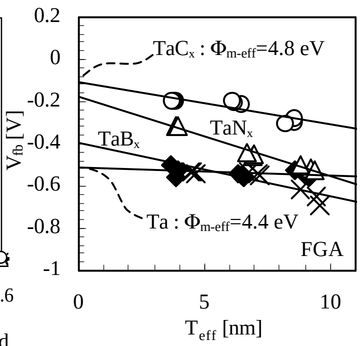

Fig. 3. V_{fb}-T_{eff} plots of Ta-based gate/SiO_2 capacitors.

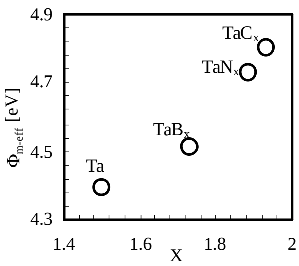

Fig. 4. Relationship between $\Phi_{m\text{-}eff}$ and electronegativities(X). For compound, the geometric mean of the constituents electronegativities is taken.

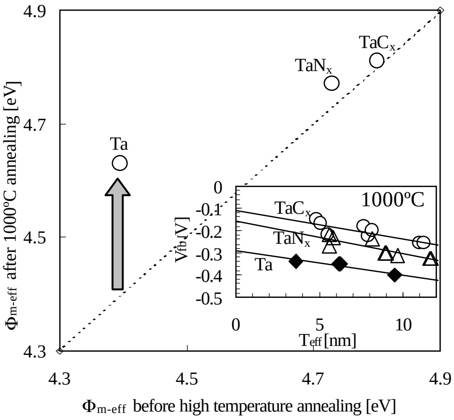

Fig. 5. Relationship between $\Phi_{m\text{-}eff}$ before and after the 1000ºC annealing. V_{fb}-T_{eff} relationships for MIS capacitors after 1000ºC annealing are also shown (inset).

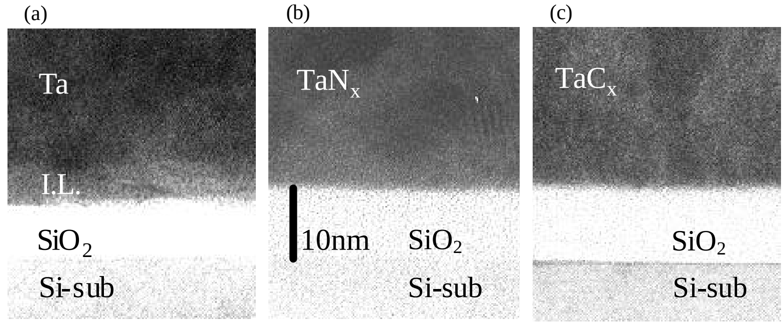

Fig. 6. Cross-sectional TEM images of (a)Ta (b)TaN_X (c)TaC_x gated MIS stacks after 1000ºC annealing. The initial thicknesses of SiO_2 before annealing are 10nm for the stack.

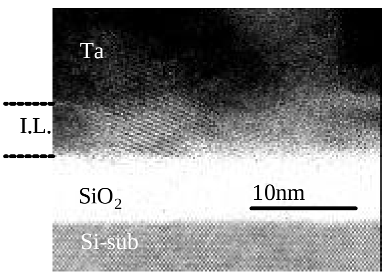

Fig. 7. Cross-sectional TEM image of Ta/SiO_2 capacitor after 1000ºC annealing.

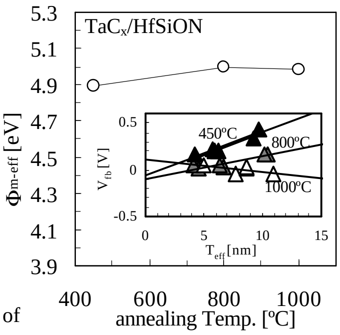

Fig. 8. V_{fb}-T_{eff} plots (inset) and thermal stability of $\Phi_{m\text{-}eff}$ for TaC_x /HfSiON capacitors.

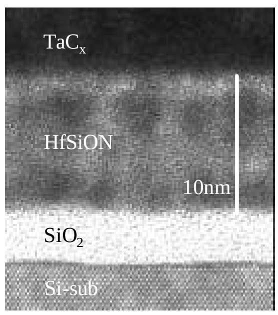

Fig. 9. Cross-sectional TEM image of TaC_X/HfSiON capacitor after 1000ºC annealing.

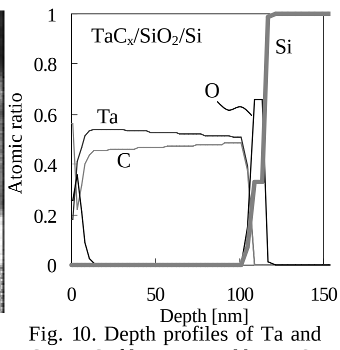

Fig. 10. Depth profiles of Ta and C in TaC_x film measured by RBS.

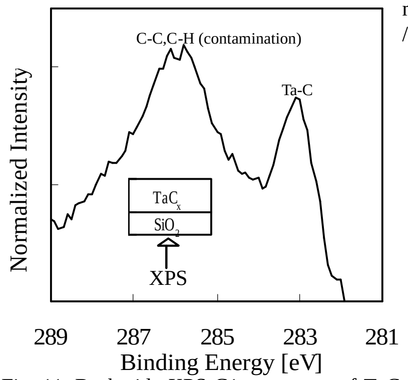

Fig. 11. Back-side XPS C1s spectrum of TaC_x gate sample at take-off angle (TOA) of 90º. C-C peaks are due to surface contamination.

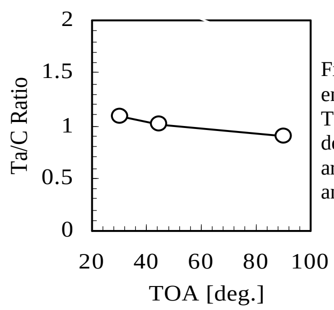

Fig. 12. The dependence of Ta/C ratio on TOA. Ta/C ratio is derived from the peak areas of Ta-C (C1s) and Ta4d spectra.

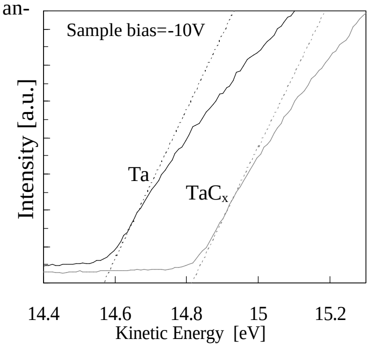

Fig. 13. Low kinetic energy cut off of UPS spectra for Ta and TaC_X.